Journal of Applied Chemistry

Green and facile synthesis of graphene supported Pt nanoparticles for oxygen reduction reaction in polymer electrolyte fuel cells

Monireh Faraji*, **Pirouz Derakhshi, Kambiz Tahvildari**

Chemistry Faculty, North Tehran Branch, Islamic Azad University, Tehran, Iran, P.O.Box . 1913674711

Abstract

In this work we report a facile and green approach to synthesis of graphene nanosheets(GNS) supported Pt nanoparticles (Pt/GNS),in which graphene acts as a high surface area and conductive host for Pt nanoparticles for oxygen reduction reaction in fuel cells. Several phytochemicals extracted from different natural leaves of plants are employed as green and eco-friendly reducing agents in the synthesis of various silver, gold, platinum, and copper nanoparticles. In this study, Cherry leaf extracts were employed as a green reducing agent to reduce graphene oxide and Pt nanoparticles. The prepared Pt/GNS exhibits greatly enhanced electrochemical performance than commercial (ElectroChem Pt/C). These are attributed to the much graphitized degree of GNS in comparison to carbon black and the improved Pt-carbon interaction in Pt/GNS,high surface area and electrical conductivity of graphene support in Pt/GNS.

1. Introduction

Polymer electrolyte fuel cells (PEFCs) are the promising power source for the future. However one of the main barriers for the commercialization of PEFCs, is the high loading of Platinum, high cost and bare noble metal, which is used as the most efficient electrocatalyst in the anode and cathode electrodes of PEFCs. As a result reducing the loading of Pt or replacing with another low cost catalyst are the main goal of researches in this field. Since particle size and agglomeration of Pt usually increase with its loading onto supports,

synthesis procedures of high-loading Pt catalyst with a narrow size distribution remains as an enormous challenge.[1-5] The size and shape of supported Pt are strongly influenced by the synthesis method, support materials and metal precursor.

In addition to the modification of the Pt catalyst by alloying with another metals, the application of suitable support is another way to improve the performance of the Pt catalyst. In the past decades, carbon materials with different morphologies have been employed for this purpose. Although the

---

***.Corresponding Author:** E-mail address m.faraji@iau-tnb.ac.ir ; Tel.: +(98)2122262563*

particular electronic interaction between carbon support and Pt catalyst has been taken into consideration, high specific area, reasonable pore structure, good conductivity and suitable anticorrosion stability are considered to be the most important features for good support[6]. It is believed that the degree of graphitization of carbon plays a key role in the durability of carbon supports, the higher degree of graphitization leads to the improved the stability.[7] In this regards a significant attention is paid to new carbon materials .Graphene is a sp^2 hybridized two dimensional monolayer of carbon. Its wide honeycomb structure is the essential building platform of other important allotropes; it can be batched to form three dimensional graphite, trilled to form one dimensional nanotubes, and wrapped to form dimension less fullerenes. High conjugation bonding system in graphene yields to outstanding mechanical, thermal and electrical properties.[8, 9] Graphene is the candidate to be used as a catalyst support in the electrocatalysis area due its high mobility of charge carriers (200,000 cm^2 V^{-1} s^{-1}) and specific surface area (calculated value, 2,630 m^2 g^{-1}).[10]

Recently in several works, the synthesis of graphene Pt nanocatalyst has been reported and remarkable effort has been dedicated to the design of new electrocatalysts supported on graphene. Seger et al. reported the fabrication of Pt nanoparticles on reduced graphene oxide sheets and used in proton exchange membrane assembly.[11] Yoo et al .prepared a new graphene supported electrocatalyst for methanol oxidation in direct methanol fuel cells.[12] Guo et al. synthesized three dimensional Pt-on-Pd bimetallic nanodendrites supported on graphene to utilize as an electrocatalyst for methanol electrooxidation.[13] Liu et al. reported the preparation of core eshell Pd@Pt dendritic nanocrystals anchored on reduced graphene oxide for methanol oxidation in fuel cells.[14]

Among the different methods for fabrication of graphene, chemical routs are the most commonly used for the production of graphene. The two essential steps in the chemical method for fabricating graphene are first the oxidation of graphite into graphene oxide and then the reduction of graphene oxide into graphene. The chemicals, conventionally used in the chemical fabrication of graphene, include hydrazine, hydroquinone, sodium borohydride, ascorbic acid, amino acids. Nevertheless, they are extremely hazardous and volatile.

In this work firstly we prepared graphene nanosheets (GNS) decorated with Platinum nanoparticles from graphite oxide (GO) using cherry leaf at temperature of 90° C as a green and eco-firendly reducing agent and then investigated its physical properties. The aim of this work is the investigation of reducing method impact on graphene physical properties and its role as a catalyst support for platinum nanoparticles as an elctrocatalyst for PEFCs electrodes.

2. Experimental procedure

2. 1. Materials and Methods

All chemicals were of analytical grade, obtained from commercial sources and used without further purification. XRD analysis was carried out operating at 40 kV out for the graphene and catalysts by using an XPERT MPD Philips diffractometer with a Cu X-ray source and 40 mA. The XRD patterns were obtained at a scanning rate of 1$^°$/min with a step size in the 2θ scan of 0.02$^°$ in the range 5-100$^°$.Structural changes in graphite ,Go and graphene were examined by using Almega Thermo Nicolet Dispersive Raman spectrometer with second harmonic @532 nm of Nd:YLF laser. The morphology of prepared catalysts were investigated by Transmission electron microscopy (TEM) using JEOL JEM 2100 F field emission electron microscope operated at 200 kV. An EG&G Princeton Applied Research Model 273A instrument and frequency response detector (model

1025) were used to define the electrochemical properties of electrodes. The efficiency of the gas diffusion electrodes (geometric exposed area 1 cm^2) for the oxygen reduction reaction was evaluated in 0.5M H_2SO_4. All measurements were carried out at 25°C in a conventional three-electrode cell, with O_2 flowing at 50 mL min^{-1}. The GDEs were put into a Teflon holder that contained a pyrolytic graphite disk as a current collector and has provision for feeding oxygen from the back of the electrode. A large area platinum flat electrode was used as the counter electrode. An Ag/AgCl reference electrode was placed close to the working electrode surface. Cyclic voltammetry were performed with a catalyst deposited glassy carbon electrode immersed in 0.5 M H_2SO_4.

2.2. Synthesis and exfoliation of GO

GO was synthesized from fine extra pure graphite powder (Merck) by the method of modified Hummers and Offeman as described elsewhere.[15, 16]

2.3. Preparation of plant leaf extracts

Cherry leafs are collected and dried for 2 days in room temperatures. The plant leaf extracts were obtained from the addition of 5 g collected and cut leaves to 100 ml boiling water .The mixture was decanted after 5 min heating and the extracts were stored in 4 ^{o}C.

2.4. In situ Reduction of graphene oxide and Pt nanoparticles

50 mg of exfoliated Go and chloroplatinic acid (H_2PtCl_6) (Aldrich) was added to round bottom and 50 mL of plant leaf extract was added drop wisely. The round bottom refluxed and heated in an oil bath at 95°C under argon atmosphere for 24 h over which the reduced GO decorated Pt gradually precipitated out as a black solid. The product has been washed

with water and methanol (100 mL) copiously, and dried in vacuum oven for 12 h in 100°C.[10]

2.5. Fabrication of the gas diffusion electrodes (GDEs)

In order to prepare the electrodes, the prepared catalysts (10wt.%), Nafion solution (Dopont)1mgcm^{-2}, glycerol (Merck), 2-propanol (Merck), and water was dispersed by means of sonication probe for 20 min. This suspension was rolled onto the carbon paper; the electrode was then dried at 400ºC for 30 min and then at 80ºC for 30 min. The Pt loading was 0.2 mg cm^{-2}.Table 1 shows prepared electrodes, GDE1-GDE2, catalyst layer features.

Table1. Fabricated electrodes properties

GDE	Catalyst	Catalyst support
GDE1	Pt/GNS	graphene
GDE2	Pt/C commercial	activated carbon (Vulcan XC-72r)

3. Results and discussion

31 XRD analyses of graphite, graphite oxide and graphene

Fig.1 shows the XRD patterns recorded for graphite, GO and reduced Graphene sample, respectively. A characteristic diffraction peak of graphite (002) appears at 26º, and the interspacing between the graphene layers is about 3.37 Å. Strong oxidation/exfoliation of graphite, leads to disruption in the ordering of the graphene layers in graphite and a smaller broader peak at 2θ=8.5º appeared for GO which corresponds to water bound intercalated oxidized graphite and oxygen functionality groups indicates the complete oxidation of graphite. The interlayer spacing between the layers is increased
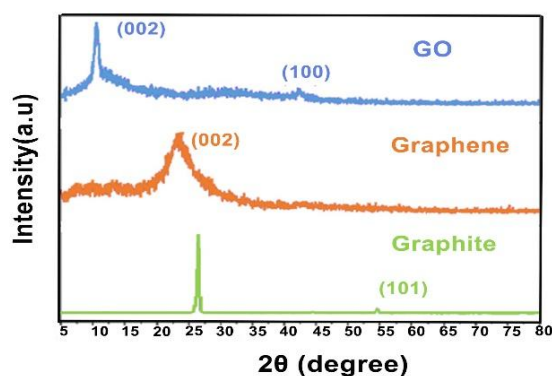
Figure 1. XRD patterns Graphite, Go, GNS

Fig2. Raman spectra of Graphite,Go and Graphenenanosheets

from 3.37 to 9 Å.[17] However, the XRD pattern of GNS does not show the diffraction peak at $2\theta = 8.5°$,the interlayer spacing of GO after reduction in GNS sample decreased, which is still a little larger than the d-spacing of well-ordered graphite (3.37A°). The small amount of functional groups and hydrogen remaining might be the main reason for this difference, indicating incomplete reduction of GO sheets to graphene [18].Table 2 shows data obtained from XRD analysis of samples. As seen in Fig.1 the (002) diffraction peak broaded in graphene samples which indicates the smaller sheet size of graphene compare to the original graphite powder and GO [19].After reduction the peak at 8.5°in the XRD spectrum is not present and broad peak is observed between 24 which is close to, but larger than, the d_{002} spacing of graphite. This indicates that functional groups remove during chemical reduction so layer number increased in graphene comparing graphite oxide but still is much lower than pristine graphite [20].

3.2. Raman spectroscopy characterization

Fig.2 shows Raman spectra of samples. In carbonaceous material, the D band and G band correspond to sp^2 and sp^3 carbon stretching modes and their intensity ratio (I_D/I_G) shows the ratio of sp^2/sp^3 carbon which is the measure of the amount of local defects and disorders.[21] Raman
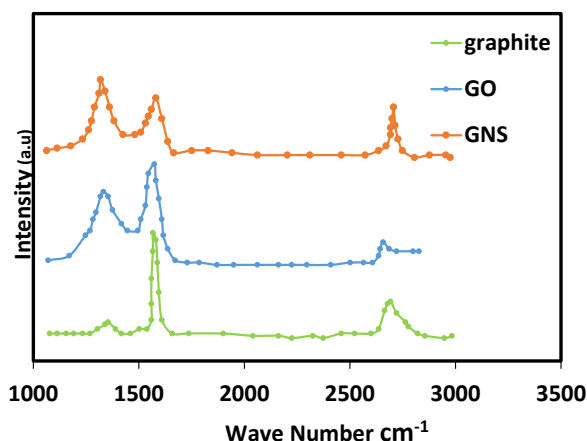
spectrum of the pristine, graphite displays a strong G band at 1579 cm^{-1}, a weak D band at 1360 cm^{-1} and a middle D´band at 2700 cm^{-1}[22].In the Raman spectrum of GO the G band broadened and shifted to 1596 cm^{-1}, In addition the D band at 1365 cm^{-1} became prominent indicating the reduction in size of the in-plane sp^2 domains possibly due to the extensive oxidation. Oxidation reaction leads to defects in GO structure and increased (I_D/I_G) ratio. After reduction this ratio decreased in graphene sheets indicating a partial restoration of the basal planes in graphene. Table 2 shows the (I_D/I_G) and $(I_G/I_D´)$ obtained from Raman spectra of samples.

Table2 Intensity ratios of Raman bands

sample	$I_{(D´/G)}$	$I_{(D/G)}$
Graphite	$5.0×10^{-1}$	$4.0×10^{-1}$
GO	$9.5×10^{-1}$	$1.0×10^{-1}$
GNS	$8.5×10^{-1}$	$5.0×10^{-1}$

The lowest (I_D/I_G) is observed for GNS which can be assigned to fewer defects in reduced graphene oxide.

3.3. XRD Analysis of Pt nanoparticles

Fig.3 shows the XRD patterns of the graphene supported Pt electrocatalysts and Pt/C (ElectroChem) electrocatalyst. The peak at $2\theta=26.5°$corresponds to the (002) planes of the graphitized graphene and the peaks at $2\theta = 39.8°$, 67.50, and 46.2°are associated
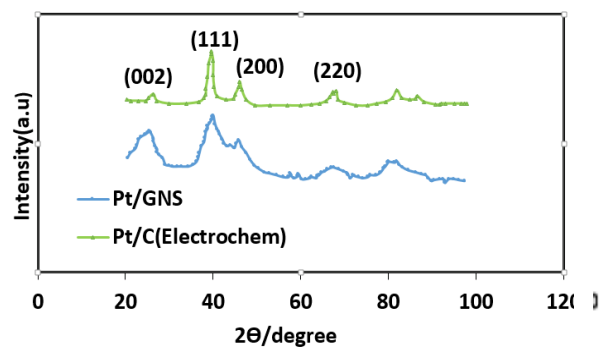
34

Figure 3. XRD pattern of Pt/GNS and Pt/C(ElectroChem)

with the (111), (220), and (200) planes of fcc (face centered cubic) Pt, respectively.[23] These results indicate that Pt has been successfully reduced on graphene host. The average sizes of the Pt particles XRD of patern of Pt/GNS and Pt/C(ElectroChem) were calculated from the line broadening of the (111) peak by using the Scherrer equation. [24] The obtained particle size were be 2.4, 1.9 Pt/C (ElectroChem) and Pt/GNS, respectively. This results revealed that Pt particles size for electrocatalyst, deposited on graphene sheets, are smaller than commercial ElectroChem Pt/C.

3.3. Morphology analysis by TEM

Fig 4 a, b, c show TEM images of graphene and platinum nanoparticles supported on GNS. In this images, platinum nanoparticles appear as dark dots with a diameter of 2 to 1.5nm on a lighter shaded substrate corresponding to the planar graphene sheet. The nanoparticles cover the graphene sheets with an interparticle distance ranging from several nanometers to several tens of nanometers, occupying only a very small portion of the surface of the graphene sheet. Pt nanoparticles aggregates can be seen only at the graphene edges where functionalized groups remained. This result also indicates a strong interaction between the functionalized graphene support and the Pt nanoparticles. The Pt nanoparticles decorated on the graphene surfaces
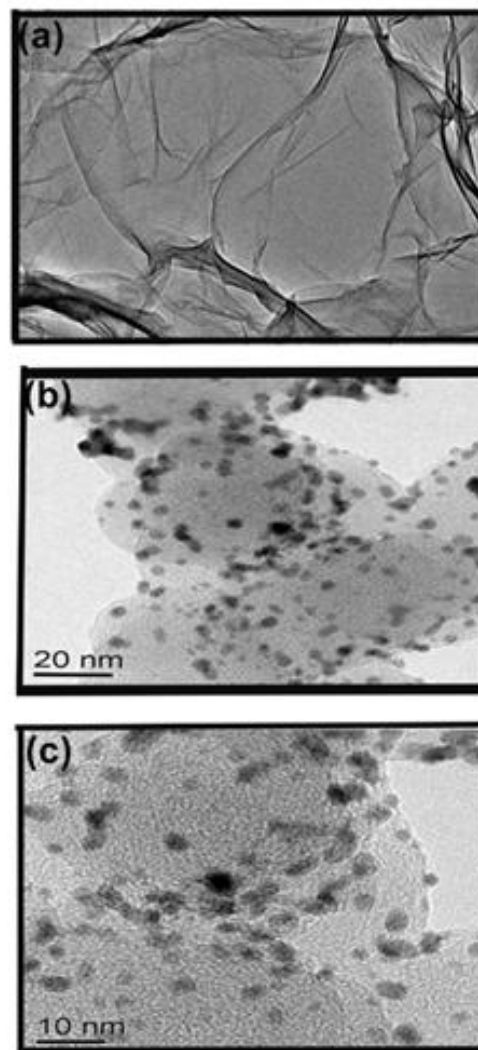

Figure 4. TEM images of graphene and Pt/GNS

can act as "spacers" to prevent the graphene from aggregation and restacking, and both faces of graphene are accessible.

3.4. Electrochemical investigations of prepared catalysts

3.4.1. Electrochemically active surface area

Cyclic voltammetry (CV) is a convenient and efficient technique used to estimate the electrochemical surface area (ECSA) of the Pt catalyst on the electrode. The CV curves for different electrocatalysts, in 0.5 M H_2SO_4 solution at a scan rate of 50mV s^{-1}are shown in Fig.5. Both CV plots
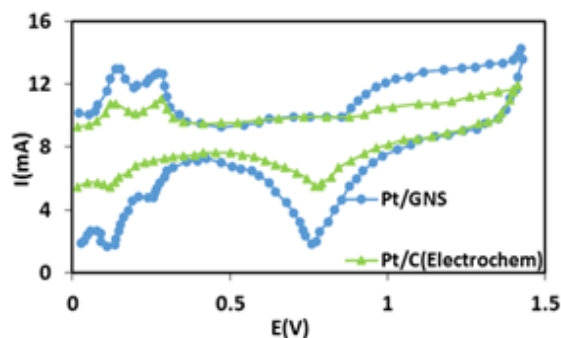
Figure5. Cyclic voltammetry curves for the GDEs for a scan rate of 50 mV s^{-1} at 25 ºC

Figure6.12 I-V curves of the GDEs in the ORR for a scan rate of 1mVs^{-1}at 25 ˚C.

show characteristic peaks for the formation and reduction of Pt oxide. In the potential region of 0.2 to 0 V (vs. Ag/AgCl), typical hydrogen adsorption and desorption peaks from polycrystalline Pt were

$$EAS = \frac{Q_h(\mu C / cm^2)}{210(\mu C / cm^2) \times [Pt](mg / cm^2)} \quad (1)$$

observed using graphene nanosheets and carbon black as supporting materials. The integrated area under the adsorption peak in the CV curves represents the total charge concerning H$^+$ adsorption, Q$_H$, and has been used to determine ECSA by employing the equation.[25]

Our calculation indicates that Pt/GNS has higher ECSA value (84m^2/g) than Pt/C (ElectroChem) (45.5m^2/g). It is due to the fact that Pt nanoparticles are smaller and more uniformly dispersed on the surfaces of Pt/graphene sheets, when compared with Pt/C. It is well known that smaller catalyst particles show higher catalytic activity. Furthermore, Pt nanoparticles dispersed on GNS surface will allow the uniform dispersion of the graphene nanosheets by reducing aggregation of the sheets, thereby producing much more accessible Pt sites for efficient catalytic activity in comparison with carbon black used as catalyst support. [26]
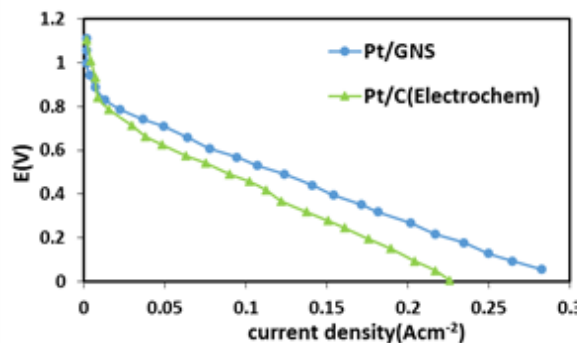
3.4.2. potentiostatic-state polarization curves

The polarization curves for the electrodes in conventional three-electrode cells are presented in Fig.6. The current density values are considerably greater for GDE1, containing Pt/GNS, than GDE2 containing commercial Pt/C (ElectroChem). The superior performance of GDE1 is attributed to increased size of the three-dimensional reaction zone and the optimum surface area of catalyst. As a result, the concentrations of the reactants near the surface of the catalyst are increased, hence the reaction rate is improved. As seen in polarization curves current densities in mass transfer region is much higher for graphene supported Pt catalyst, than commercial activated carbon (Vulcan XC72r) supported Pt/C (ElectroChem) which is related to the different porous structure of graphene and carbon black. Mesopore sizes in graphene facilitated water transport in electrode which leads to the better proton transfer and prevents mass transfer limitation, besides presence of micro pores in graphene structure allows oxygen accessibility to electrode surface.[27] The kinetic parameters of the ORR for a GDE can be obtained from the polarization data. Our analysis of the experimental

$$E_{rev} - E = b \log i / i_0 \quad (2)$$

36

polarization data was performed by using the Tafel equation:[28]

where E_{rev}, E,b,I,i_0 are reaction equilibrium potential, reaction potential, Tafel slope, current density and exchange current density,respectively. The electrochemical parameters, Table 3, derived from Tafel equation.

Table 3 Kinetic parameters obtained from polarization curve for

GDE	Tafel slope(mvdec^{-1})	i_0(Acm^{-2})
GDE1	73.34	3.90×10^{-5}
GDE2	90.00	3.60×10^{-5}

The best kinetic parameters are observed for GDE1 (Pt/GNS) catalyst. This results show that surface area, and morphology are optimum for GNS in comparison with Vulcan XC-72r makes it better catalyst support for Pt to catalyze oxygen reduction reaction.

3.4.3. Choronoampermetrye

Choronoamperometry is employed to determine to the diffusion coefficient of oxygen to the catalyst layer of electrodes. Diffusion coefficient, seen in Table 4, can be obtained from modified Cottrel equation.

$$i(t) = \left(nFAD^{1/2}C\right)\left(\pi^{1/2}t^{1/2}\right) + nFADC/r \quad (3)$$

where r is the diameter of the electrode, i is the limiting current (mA); n is the number of electrons, F is the columbic charge (964850 C mol^{-1}), D is the diffusion coefficient (Cm^{2}s^{-1}), t is the time (s), and C* is the

Table 4 permeability of oxygen to electrode

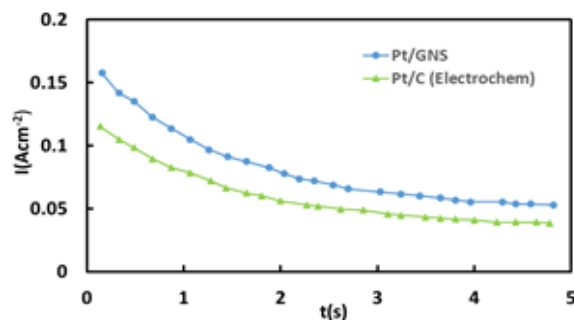| GDE	(D$^{(1/2)}\times$C*)10^{-8} (molcm^{2}s$^{-1/2}$)
GDE1	6.75
GDE2	3.50

Figure7. Chronoamperograms of the GDEs in the presence of O$_2$, E 0.4 V vs. Ag/AgCl, at 25°C.

saturated concentration of oxygen in sulfuric acid (1.38×10^{-6} mM). As seen in Fg.7 and table 4 GDE1 (Pt/GNS) exhibits the higher permeability, It is may be due to the modified porous structure of GNS. The presence of micro pores in GNS increased gas permeability and oxygen diffusion toward

the catalyst, whereas mesoporous structure of (Vulcan XC-72r) in GDE1, act weakly for gas diffusion. Micropore structure of carbon support which involved with gas has a crucial role in mass transport for liquid face. As a result it seems that the presence of both macropores and micropores in oxygen reduction reaction which occurs in the interface of liquid(proton transport) and gas phase(oxygen permeability) are necessary to enhance the catalyst performance.[29]

4. Conclusion

A quick, simple, inexpensive and an environmental-friendly preparation of the graphene supported Pt nanoparticles by cherry leaf was reported in this work. Pt nanoparticles were deposited on GNS sample and the activity of prepared catalyst is examined for oxygen reduction reaction. The morphological investigations revealed that there is a strong interactions between Pt nanoparticles and graphene and graphene act as a high surface area and conductive platform for Pt nanoparticles.The graphene supported catalyst (Pt/GNS) has better performance than commercial

ElectroChem Pt/C. These results indicate that graphene nanosheets could be a good candidate as a supporting material of electrocatalysts of fuel cells electrodes.

References

[1]   K. Okaya, H. Yano, H. Uchida, M. Watanabe, ACS Applied Materials and Interfaces 2 (2010) 888-895.

[2]   B. Guenot, M. Cretin, C. Lamy, J Appl Electrochem 45 (2015) 973-981.

[3]   H. Gharibi, M. Faraji, M. Kheirmand, Electroanalysis 24 (2012) 2354-2364.

[4]   A. Heydari, H. Gharibi, J Power Sources 325 (2016) 808-815.

[5]   H. Gharibi, F. Yasi, M. Kazemeini, A. Heydari, F. Golmohammadi, RSC Adv. 5 (2015) 85775-85784.

[6]   س.س. تقوی, ع. اصغری, ا. توسلی, شیمی کاربردی ۱۱ (۲۰۱٦) ۱۲۹-۱۳۸.

[7]   L. Zhao, Z.B. Wang, J.L. Li, J.J. Zhang, X.L. Sui, L.M. Zhang, J. Mater. Chem. A 3 (2015) 5313-5320.

[8]   M.J. Allen, V.C. Tung, R.B. Kaner, Chemical Reviews 110 (2010) 132-145.

[9]   X. Gao, J. Jang, S. Nagase, Journal of Physical Chemistry C 114 (2010) 832-842.

[10]   H.J. Shin, K.K. Kim, A. Benayad, S.M. Yoon, H.K. Park, I.S. Jung, M.H. Jin, H.K. Jeong, J.M. Kim, J.Y. Choi, Y.H. Lee, Advanced Functional Materials 19 (2009) 1987-1992.

[11]   B. Seger, P.V. Kamat, Journal of Physical Chemistry C 113 (2009) 7990-7995.

[12]   E. Yoo, T. Okata, T. Akita, M. Kohyama, J. Nakamura, I. Honma, Nano Letters 9 (2009) 2255-2259.

[13]   S. Guo, S. Dong, E. Wang, ACS Nano 4 (2010) 547-555.

[14]   Q. Liu, Y.R. Xu, A.J. Wang, J.J. Feng, Journal of Power Sources 302 (2016) 394-401.

[15]   W.S. Hummers Jr, R.E. Offeman, Journal of the American Chemical Society 80 (1958) 1339.

[16]   Z.S. Wu, W. Ren, L. Gao, B. Liu, C. Jiang, H.M. Cheng, Carbon 47 (2009) 493-499.

[17]   H.M. Ju, S.H. Choi, S.H. Huh, Journal of the Korean Physical Society 57 (2010) 1649-1652.

[18]   J. Yan, T. Wei, B. Shao, F. Ma, Z. Fan, M. Zhang, C. Zheng, Y. Shang, W. Qian, F. Wei, Carbon 48 1731-1737.

[19]   C.V. Rao, A.L.M. Reddy, Y. Ishikawa, P.M. Ajayan, Carbon 49 931-936.

[20]   J. Yan, T. Wei, B. Shao, F. Ma, Z. Fan, M. Zhang, C. Zheng, Y. Shang, W. Qian, F. Wei, Carbon 48 (2010) 1731-1737.

[21]   Y.H. Ding, P. Zhang, Q. Zhuo, H.M. Ren, Z.M. Yang, Y. Jiang, Nanotechnology 22 (2011).

[22]   A.C. Ferrari, Solid State Communications 143 (2007) 47-57.

[23]   H. Huang, H. Chen, D. Sun, X. Wang, Journal of Power Sources 204 (2012) 46-52.

[24]   H. Gharibi, M. Javaheri, M. Kheirmand, R.A. Mirzaie, International Journal of Hydrogen Energy In Press, Corrected Proof.

[25]   A. Pozio, M. De Francesco, A. Cemmi, F. Cardellini, L. Giorgi, Journal of Power Sources 105 (2002) 13-19.

[26]   Y. Li, W. Gao, L. Ci, C. Wang, P.M. Ajayan, Carbon 48 (2009) 1124-1130.

[27]   T. Soboleva, K. Malek, Z. Xie, T. Navessin, S. Holdcroft, ACS Applied Materials and Interfaces 3 (2011) 1827-1837.

[28]   J.   Zhang,   PEM   Fuel   Cell Electrocatalysts   and   Catalyst   Layers Fundamentals   and   Applications,   Springer-, london, 2008.

[29]   Y. Liu, C. Ji, W. Gu, J. Jorne, H.A. Gasteiger, Journal of the Electrochemical Society 158 (2011) B614-B621.